

## Studies on anticancer properties with varying co-ligands in Ru(II) arene benzimidazole system

Pragti<sup>1‡</sup>, Sreshtha Nayek<sup>1‡</sup>, Satyam Singh<sup>2</sup>, Avinash Sonawane<sup>2</sup>, Ivo Grabchev<sup>3</sup>, Rakesh Ganguly<sup>4</sup>, Suman Mukhopadhyay<sup>1\*</sup>

<sup>1</sup>Department of Chemistry, School of Basic Sciences, Indian Institute of Technology Indore, Simrol, Khandwa Road, Indore, 453552, India

<sup>2</sup> Department of Biosciences and Biomedical Engineering, Indian Institute of Technology Indore, Madhya Pradesh 453 552, India

<sup>3</sup>Sofia University “St Kliment Ohridski” Faculty of Medicine, 1, Koziak Str., 1407 Sofia, Bulgaria

<sup>4</sup>Shiv Nadar University, Greater Noida, 201314, India

\*E-mail: [suman@iiti.ac.in](mailto:suman@iiti.ac.in); Tel: +91 731660 3328

‡ = Contributed equal authorship

### Table of Contents

Entry	Content	Page no.
<b>Section S1</b>	Abbreviations	03
<b>Section S2</b>	Experimental Section	04
<b>Section S3</b>	<b>Experimental Methods</b>	<b>04-07</b>
<b>Section S3.1</b>	Lipophilicity Study	04
<b>Section S3.2</b>	Protein Binding study	05
<b>Section S3.3</b>	DNA binding study	05
<b>Section S3.4</b>	Cytotoxicity assay	06
<b>Section S3.5</b>	Cell imaging study	07
<b>Section S4</b>	<b>Figures</b>	<b>08-24</b>
<b>Figure S1</b>	NMR spectra of ligand (HL) in DMSO-d <sub>6</sub> (a) <sup>1</sup> H NMR (b) <sup>13</sup> C NMR	08
<b>Figure S2</b>	NMR spectra of complex <b>1</b> in DMSO-d <sub>6</sub> (a) <sup>1</sup> H NMR (b) <sup>13</sup> C NMR	09
<b>Figure S3</b>	NMR spectra of complex <b>2</b> in DMSO-d <sub>6</sub> (a) <sup>1</sup> H NMR (b) <sup>13</sup> C NMR (c) <sup>31</sup> P NMR	10-11
<b>Figure S4</b>	NMR spectra of complex <b>3</b> in DMSO-d <sub>6</sub> (a) <sup>1</sup> H NMR (b) <sup>13</sup> C NMR (c) <sup>31</sup> P NMR	11-12
<b>Figure S5</b>	ESI-MS of ligand (HL)	13
<b>Figure S6</b>	ESI-MS of complex <b>1</b>	13

<b>Figure S7</b>	ESI-MS of complex <b>2</b>	13
<b>Figure S8</b>	ESI-MS of complex <b>3</b>	14
<b>Figure S9</b>	FTIR stretching frequencies (in KBr pellet) of (a) ligand ( <b>HL</b> ), (b) complex <b>1</b> , (c) complex <b>2</b> , and (d) complex <b>3</b>	14
<b>Figure S10</b>	(a) UV-Visible spectra (b) emission spectra of ligand ( <b>HL</b> ) and complexes <b>1-3</b> in DMSO	15
<b>Figure S11</b>	Time dependent stability study of complex <b>1</b> at different time intervals 0 hr, 24 hr, 48 hr using NMR spectroscopy.	15
<b>Figure S12</b>	Time dependent stability study of complex <b>2</b> at different time intervals 0 hr, 24 hr, 48 hr using NMR spectroscopy.	16
<b>Figure S13</b>	Time dependent stability study of complex <b>3</b> at different time intervals 0 hr, 24 hr, 48 hr using NMR spectroscopy	16
<b>Figure S14</b>	Stability study of the (a) complex <b>1</b> , (b) complex <b>2</b> , and (c) complex <b>3</b> (in 1% DMSO in PBS Solution) using UV spectroscopy	17
<b>Figure S15</b>	Stability study of complexes in DMEM Media (a) complex <b>1</b> (b) complex <b>2</b> (c) complex <b>3</b> at different time interval 0 hr, 24 hr, 48 hr (in DMEM).	17
<b>Figure S16</b>	Stability study of complex <b>1</b> in DMEM Media at different time intervals 0 hr, 24 hr, 48 hr via LC-MS.	18
<b>Figure S17</b>	Stability study of complex <b>2</b> in DMEM Media at different time intervals 0 hr, 24 hr, 48 hr via LC-MS.	19
<b>Figure S18</b>	Stability study of complex <b>3</b> in DMEM Media at different time interval 0 hr, 24 hr, 48 hr via LC-MS.	20
<b>Figure S19</b>	Fluorescence quenching spectra of HSA (10 $\mu$ M) of (a) ligand ( <b>HL</b> ), (b) complex <b>1</b> , (c) complex <b>2</b> , and (d) complex <b>3</b> (2-20 $\mu$ M) at 298 K.	21
<b>Figure S20</b>	Fluorimetric titration spectra of BSA (10 $\mu$ M) in Tris-HCl buffer with (a) ligand ( <b>HL</b> ), (b) complex <b>1</b> , (c) complex <b>2</b> , and (d) complex <b>3</b> (2-20 $\mu$ M) at 298 K. Inset: Stern-Volmer plots for BSA.	22
<b>Figure S21</b>	Absorption titration spectra of (a) ligand ( <b>HL</b> ), (b) complex <b>1</b> , (c) complex <b>2</b> , and (d) complex <b>3</b> with increasing concentrations of CT-DNA	23

<b>Figure S22</b>	Normalized log of concentrations of the doses of ligand ( <b>HL</b> ) and complexes <b>1-3</b> against (a) HeLa, (b) MCF7 (cancer cell lines) and (c) HEK 293 (normal cell line)	23
<b>Figure S23</b>	Cell viability curve for ligand ( <b>HL</b> ) and complexes <b>1-3</b> against cancer cell lines (a) HeLa, (b) MCF-7 and (c) normal cell line HEK 293	24
<b>Figure S24</b>	(a) Generation of reactive oxygen species after the treatment of complexes in HeLa cells (b) Histogram graph of ROS fluorescence intensity	24
<b>Section S5</b>	<b>Tables</b>	<b>25-27</b>
<b>Table S1</b>	Selected bond lengths (Å) and bond angles (°) of complexes <b>1</b> and <b>2</b>	25-26
<b>Table S2</b>	Excitation and emission wavelengths of ligand ( <b>HL</b> ) and complexes <b>1-3</b>	26
<b>Table S3</b>	Various binding parameters analyzed from SV and Scatchard plots	26
<b>Table S4</b>	IC <sub>50</sub> values obtained from MTT assay of the ligand ( <b>HL</b> ) and complexes <b>1-3</b> against cancer cell lines (HeLa and MCF-7) along with a comparison with normal cell line (HEK 293).	27
<b>Section S6</b>	<b>References</b>	<b>27</b>

## Section S1. Abbreviation used in this article

Entry	Significance	Entry	Significance
<b>NMR</b>	Nuclear magnetic resonance	<b>DAPI</b>	4',6-diamidino-2-phenylindole
<b>ESI-MS</b>	Electrospray ionisation mass spectrometry	<b>UV-Vis</b>	Ultraviolet-Visible
<b>FTIR</b>	Fourier transformed infra-red	<b>r.t.</b>	Room temperature
<b>CT-DNA</b>	calf thymus deoxyribonucleic acid	<b>FL</b>	Fluorescence
<b>MTT</b>	3-(4,5-dimethylthiazol-2-yl)-2,5-diphenyl tetrazolium bromide	<b>PBS</b>	Phosphate Buffered Saline

## Section S2. Experimental Section

### Instrumentation

All the chemicals required are purchased from Sigma and used without further purification. Chemicals for biological experiments (3-(4,5-dimethylthiazol-2-yl)-2,5-diphenyltetrazolium bromide (MTT), PBS buffer were purchased from Himedia chemical, India. An AVANCE III 400 Ascend Bruker BioSpin spectrometer was used to record  $^1\text{H}$  and  $^{13}\text{C}$  NMR spectroscopy at room temperature. Infrared (FTIR) spectra (range: 4000 to 500  $\text{cm}^{-1}$ ) was conducted on BRUKER TENSOR 27 instrument. Elemental analyses (C, H, N and S content) were performed with a MicroTOF-Q II mass spectrometer and ThermoFlash 2000 elemental analyzer. ESI-MS were carried out on Bruker-Daltonics. Spectrophotometric measurements for absorption study were done by using a quartz cuvette with a path length of 1 cm on a Varian UV-Vis spectrophotometer (Model: Cary 100). A Perkin-Elmer lambda-650 DRS UV-Vis spectrophotometer, equipped with an integration sphere diffuse reflectance attachment in the range of 200-1200 nm against  $\text{BaSO}_4$  as reference was utilized for UV-Vis diffuse reflectance spectral (UV-Vis/ DRS) analyses. The far-ultraviolet (UV) (190 to 260 nm) spectra were recorded in 0.1 cm path length cell (Hellma, Muellheim/Baden, Germany) using a step size of 0.5 nm, bandwidth of 1 nm and a scan rate of 20  $\text{nm min}^{-1}$ . Fluorescence emission spectra were recorded at  $25.0 \pm 0.2$  °C on a Fluoromax-4p spectrofluorometer from Horiba JobinYvon (Model: FM-100) using a quartz cuvette with a path length of 2 cm. Conductivity measurements were performed using a Digital Conductivity Meter Model 611 instrument. The conductivities of the complexes were obtained with 1 mM solutions in DMSO. Staining assay were done with the help of confocal microscope Fluoview FV100 (OLYMPUS, 449 Tokyo, Japan).

### **Section S3. Experimental Methods**

#### **S3.1 Lipophilicity Study**

The lipophilicity ( $\log P$ ) of complexes was measured using the shake-flask procedure in 1-octanol ( $\text{CH}_3(\text{CH}_2)_7\text{OH}$ ) and pure water (HPLC grade). Initially, the optical densities of the complexes were measured separately at three different concentrations in both octanol and a mixture of water and DMSO (2:1) (due to poor solubility in water). From a plot of absorbance vs. concentration, the slope was used to determine the extinction coefficient. 5 mg of the compounds were taken in a solution comprising of 10 mL water and 10 mL octanol. The two phases were shaken for 5–30 minutes at room temperature and left to equilibrate for 24 h. After standing, 1 mL of the complex in both the phases was extracted and the concentration was measured spectrophotometrically, using Lambert Beer's law from the absorbance of the spectra obtained.<sup>1</sup>  $P_{\text{o/w}}$  value was calculated according to the equation

$$P_{\text{o/w}} = \text{concentration in octanol} / \text{concentration in water} \quad (1)$$

#### **S3.2 Protein Binding Study - Competitive binding experiments**

Protein binding studies of the synthesized compounds were carried out by tryptophan fluorescence quenching experiments using human serum albumin (HSA) and bovine serum albumin (BSA). The excitation wavelength for HSA and BSA was at 280 nm, and the quenching of the emission intensity of the tryptophan residues of the proteins at 345 nm was monitored using the complexes as a quencher with increasing concentration. The excitation and emission slit widths and scan rates were kept constant throughout the experiment. A 10  $\mu$ M stock solution of BSA/HSA was prepared using 50 mM tris buffer solution and stored at 4 °C for further use. Stock solutions of 5 mM strength were made using synthesized compounds. Fluorometric titration was carried out taking 2 mL of the protein solution and the fluorescence intensity was measured as blank. For titration, each time, 2  $\mu$ L of the stock solution was added to the protein solution and the fluorescence intensity was measured. For all the four complexes, up to 20  $\mu$ L of the solution was added to measure fluorescence quenching. The fluorescence quenching data were further analyzed by using the Stern–Volmer equation, which again can be expressed in terms of the bimolecular quenching rate constant and the average life time of the fluorophore as shown in the following equation:

$$F_0/F = 1 + K_{sv} [Q] = 1 + K_q \tau_0 [Q] \dots (2)^2$$

where  $F_0$  and  $F$  are the fluorescence intensities in the absence and presence of a quencher,  $K_q$  is the bimolecular quenching rate constant,  $\tau_0$  is the average lifetime of a fluorophore in the absence of a quencher and  $[Q]$  is the concentration of a quencher (metal complexes).  $K_{SV}$  is the Stern–Volmer quenching constant in  $M^{-1}$ . The binding constant  $K_a$  and number of complex bound to BSA/HSA ( $n$ ) are calculated using the following formula.

$$\log [(F_0 - F)/F] = \log K_a + n \log [Q] \dots (3)^3$$

The magnitudes of  $K_a$  and  $K_q$  of complexes are  $10^6 M^{-1}$  and  $10^{13} M^{-1}s^{-1}$ , respectively, indicating a good binding ability to serum protein.

### **S3.3 DNA binding study**

#### **S3.3.1 Competitive binding experiments**

The relative binding of complex to CT-DNA were determined with a DAPI-bound CT-DNA solution in Tris-HCl/ NaCl buffer (5 mM/ 50 mM, pH=7.4). DNA was pre-treated with DAPI for 30 min by maintaining the fixed ratio of  $[DNA]/[DAPI] = 2.0$ . The fluorescence quenching effect on addition of complex to the DAPI-DNA complex have been analyzed by recording the fluorescence emission spectra with excitation at 350 nm and emission at 458 nm. The titration quenching experiment was carried out by keeping the concentration of DNA in buffer constant ( $[CT-DNA] = 10 \mu M$  and  $[dye] = 15 \mu M$ ) and adding the sample

solution within the concentrations range of 0-100  $\mu\text{M}$ . After addition of the sample solution, the solution was kept for 1 min and then fluorescence intensity was measured.<sup>2</sup>

### **S3.3.2 Absorption spectral studies**

The interaction between metal complexes and DNA were studied using electronic absorption method. Disodium salt of calf thymus CT-DNA was stored at 4 °C. Solution of CT-DNA in the buffer 50 mM NaCl/ 5 mM Tris (pH 7.2) in water gave a ratio 1.9 of UV absorbance at 260 and 280 nm ( $A_{260}/A_{280}$ ,  $A$  = absorbance), indicating that the DNA was sufficiently free from protein. The concentration of DNA was measured using its extinction coefficient ( $\epsilon$ ) at 260 nm after 1:100 dilutions. Stock solutions were stored at 4°C and used for not more than 4 days. Concentrated stock solutions of the complexes were prepared by dissolving the complexes in DMSO and diluting suitably with the corresponding buffer to the required concentration for all of the measurements. Absorption spectra titrations were performed at room temperature in Tris HCl/ NaCl buffer (5 mM/ 50 mM buffer, pH 7.4) to investigate the binding affinity between CT-DNA and complex. A fixed concentration of the complex (10  $\mu\text{M}$ ) was titrated with increasing amounts of CT-DNA concentration (0-150  $\mu\text{L}$ ). The intrinsic binding constant for the interaction of complex with CT-DNA was obtained from absorption spectral data.<sup>2</sup>

### **S3.4 Cytotoxicity assay**

The cell line was obtained from the National Centre for Cell Sciences (NCCS) Pune, India. It was cultured in the Dulbecco's Modified Eagles medium (DMEM) supplemented with 10% fetal bovine serum (FBS), 200 mM L-glutamine, 100  $\mu\text{g/mL}$  penicillin, and 10 mg/mL streptomycin in a humidified atmosphere consisting of 5 %  $\text{CO}_2$  at 37°C. Cells were cultured and maintained in logarithmic growth phase until number of cells reaches at  $1.0 \times 10^6$  cells/mL.

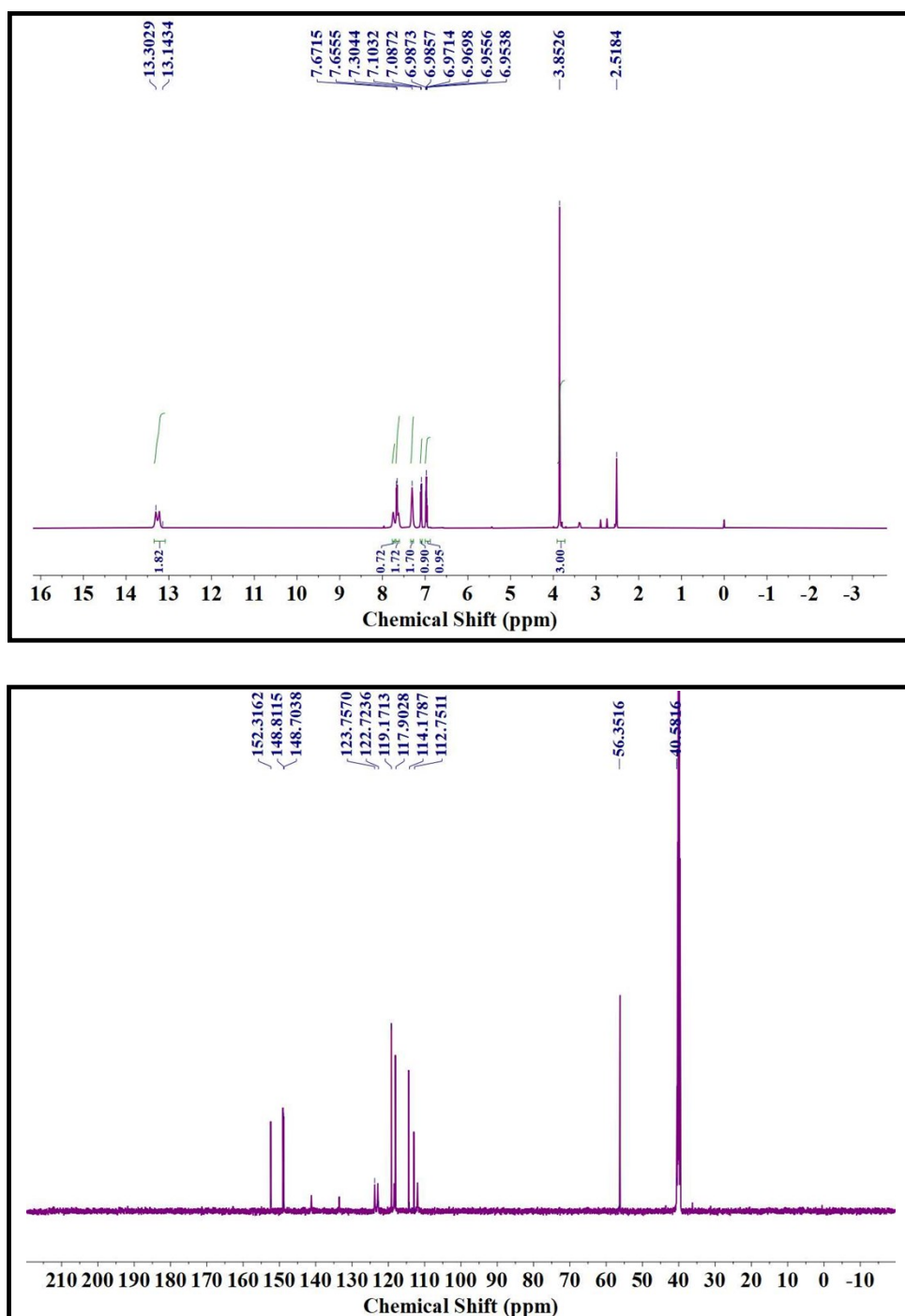
#### **S3.4.1 Evaluation of cytotoxicity**

The cytotoxic effect of complex against HeLa and MCF-7 cells was evaluated by MTT [3-(4, 5-dimethylthiazol-2-yl)-2, 5-diphenyltetrazoliumbromide] assay. Briefly, all cells were seeded ( $5 \times 10^4$  cells/well) in a 96-well plate and kept in  $\text{CO}_2$  for attachment and growth for 24 h. Then, the cells were treated with various concentrations of complex dissolved in DMSO or water (0.25-100  $\mu\text{M}$ ) and incubated for 24 h. After incubation, the culture medium was removed and 10  $\mu\text{L}$  of MTT solution (5 mg/mL in PBS) was added to each well. Following 4 h incubation in dark, MTT was discarded and DMSO or water (100  $\mu\text{L}$ /well) was added to solubilize the purple formazan product. The experiment was carried out in triplicates and the medium without complex served as control. The absorbance was measured colorimetrically at 570 nm using an ELISA microplate reader. The percentage of cell viability was calculated using the following formula and expressed as: % cell viability = (OD value of treated cells)/ (OD value of untreated cells

(control)  $\times 100$ .<sup>2,4</sup> The cytotoxic concentration/ dose that killed 50 % of the cells ( $IC_{50}$ ) was determined from the absorbance (OD) versus concentration linear regression curve using Prism GraphPad software package. Each well was triplicated and each experiment repeated at least three times.  $IC_{50}$  values quoted are mean  $\pm$  SEM.

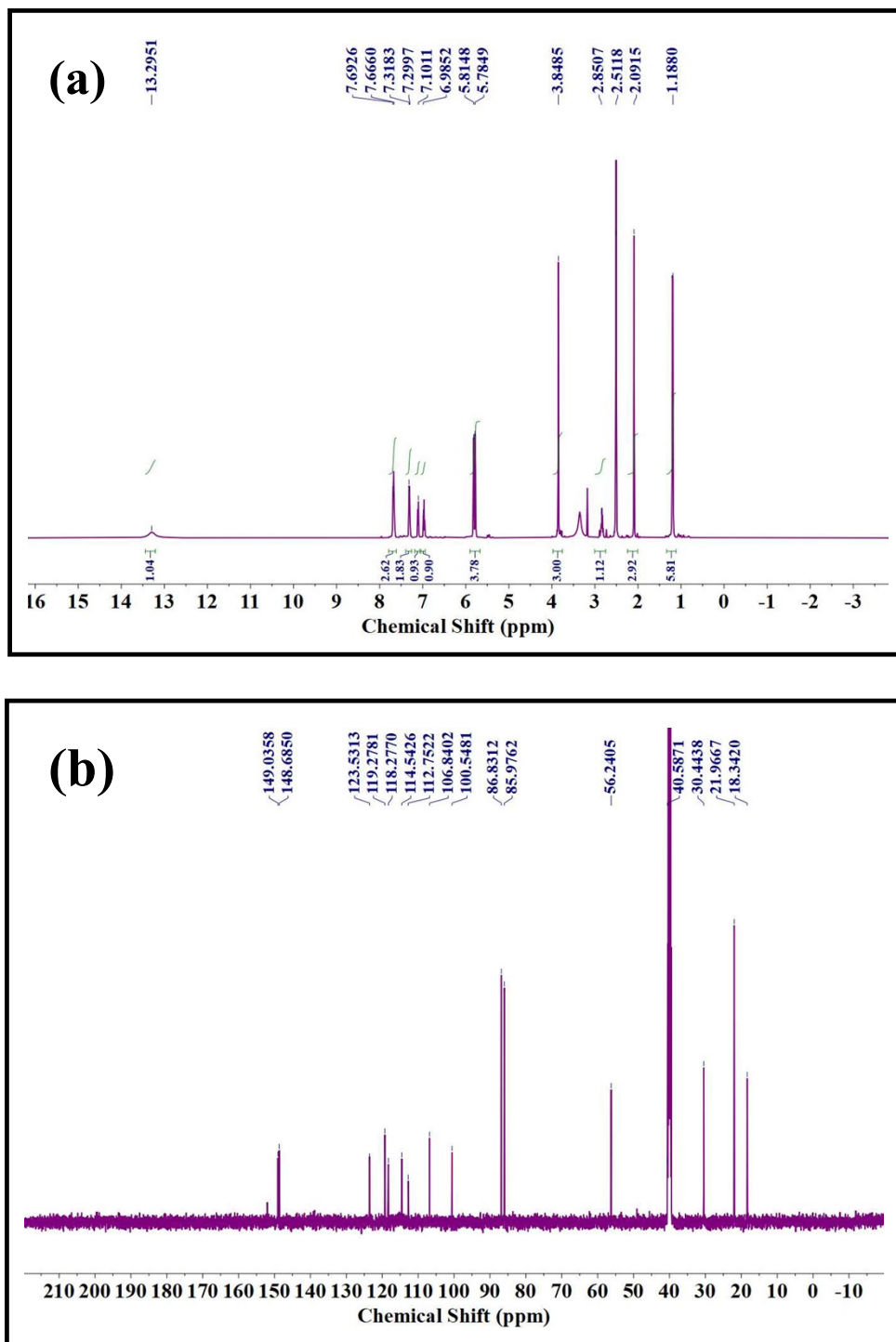
### **S3.5 Cell imaging study**

$5 \times 10^4$  HeLa cells were placed in six-well plates having a coverslip in each well and were incubated overnight in the  $CO_2$  incubator for attachment. The cells were then treated with corresponding  $IC_{50}$  concentration of complexes 3 and 4 for 24 h and untreated cells were taken as control stained with Hoechst stain 33258. These cells were then fixed with 4% paraformaldehyde followed by permeabilization with 0.1% Triton x 100. Untreated cells were now stained with 5  $\mu$ g/mL Hoechst 33258 for 30 min at room temperature followed by washing with PBS buffer. Then the coverslips were mounted on glass slides, and the fluorescence was viewed under OLYMPUS confocal microscope.<sup>5, 6</sup>

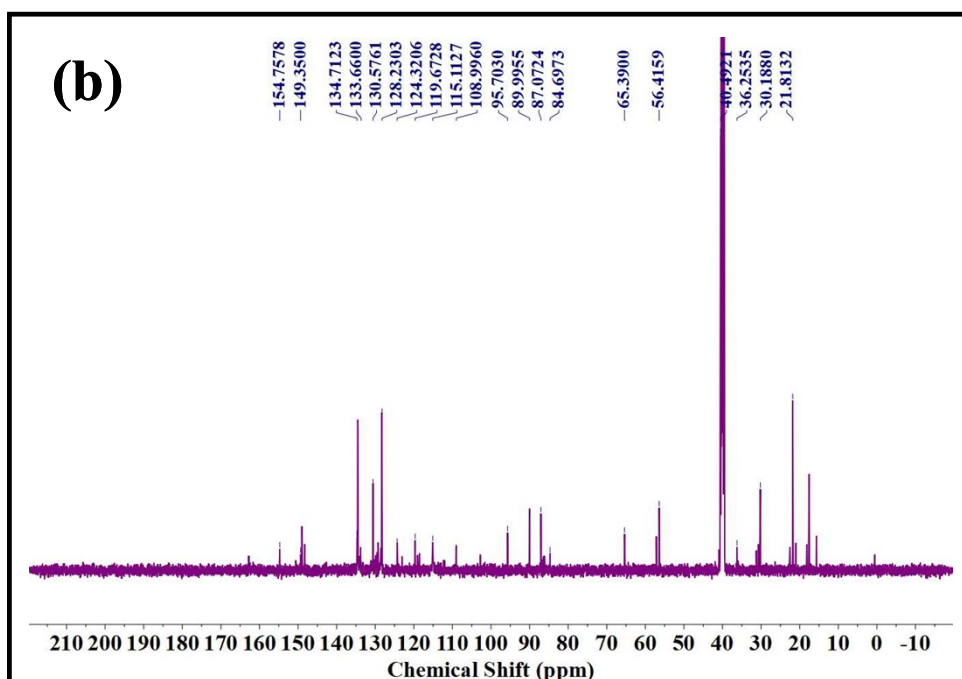
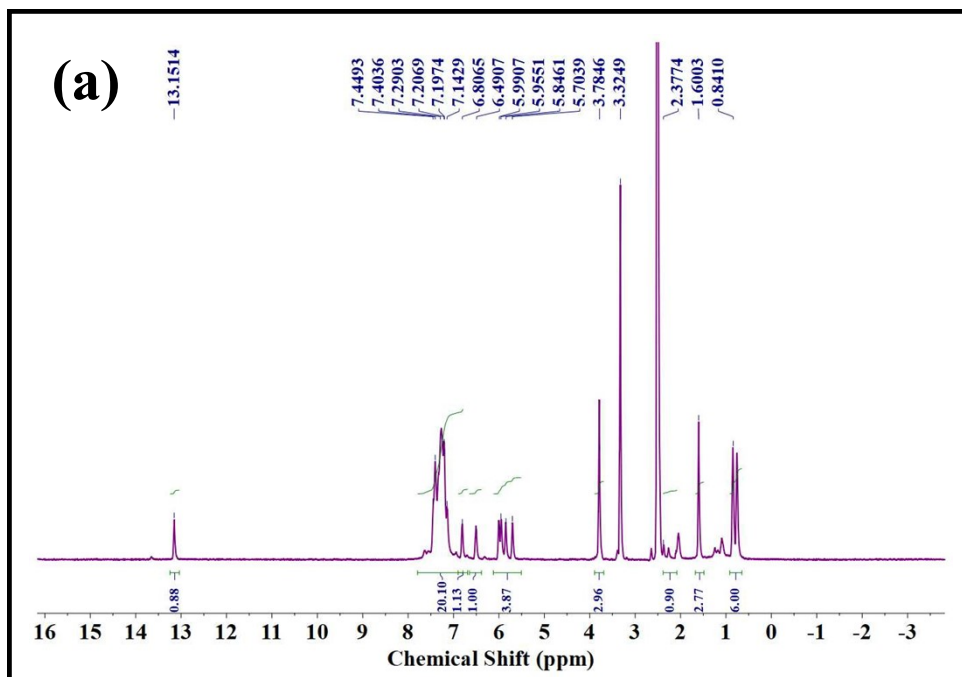


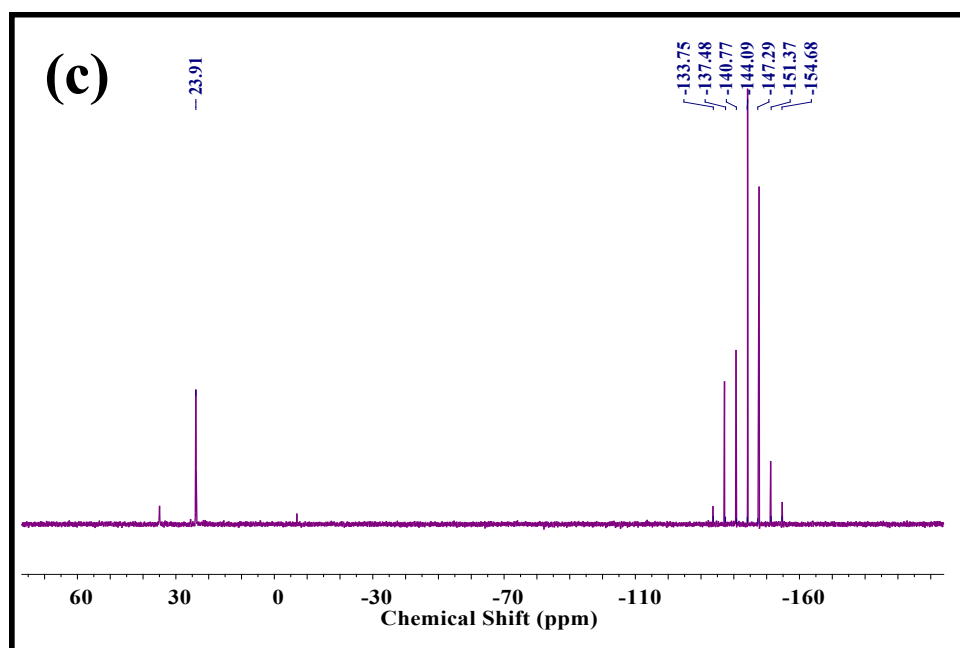
**Figure S1:** NMR spectra of ligand (**HL**) in DMSO- $\text{d}_6$  (a)  $^1\text{H}$  NMR (b)  $^{13}\text{C}$  NMR



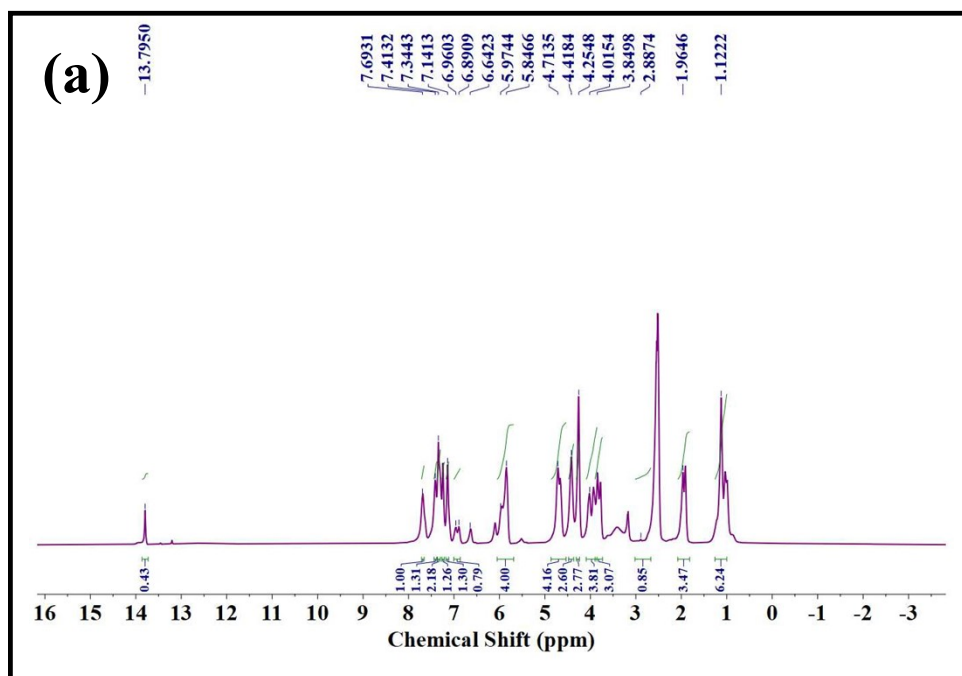


**Figure S2:** NMR spectra of complex **1** in DMSO- $d_6$  (a)  $^1\text{H}$  NMR (b)  $^{13}\text{C}$  NMR





**Figure S3:** NMR spectra of Complex **2** in DMSO- $d_6$  (a)  $^1\text{H}$  NMR (b)  $^{13}\text{C}$  NMR (c)  $^{31}\text{P}$  NMR



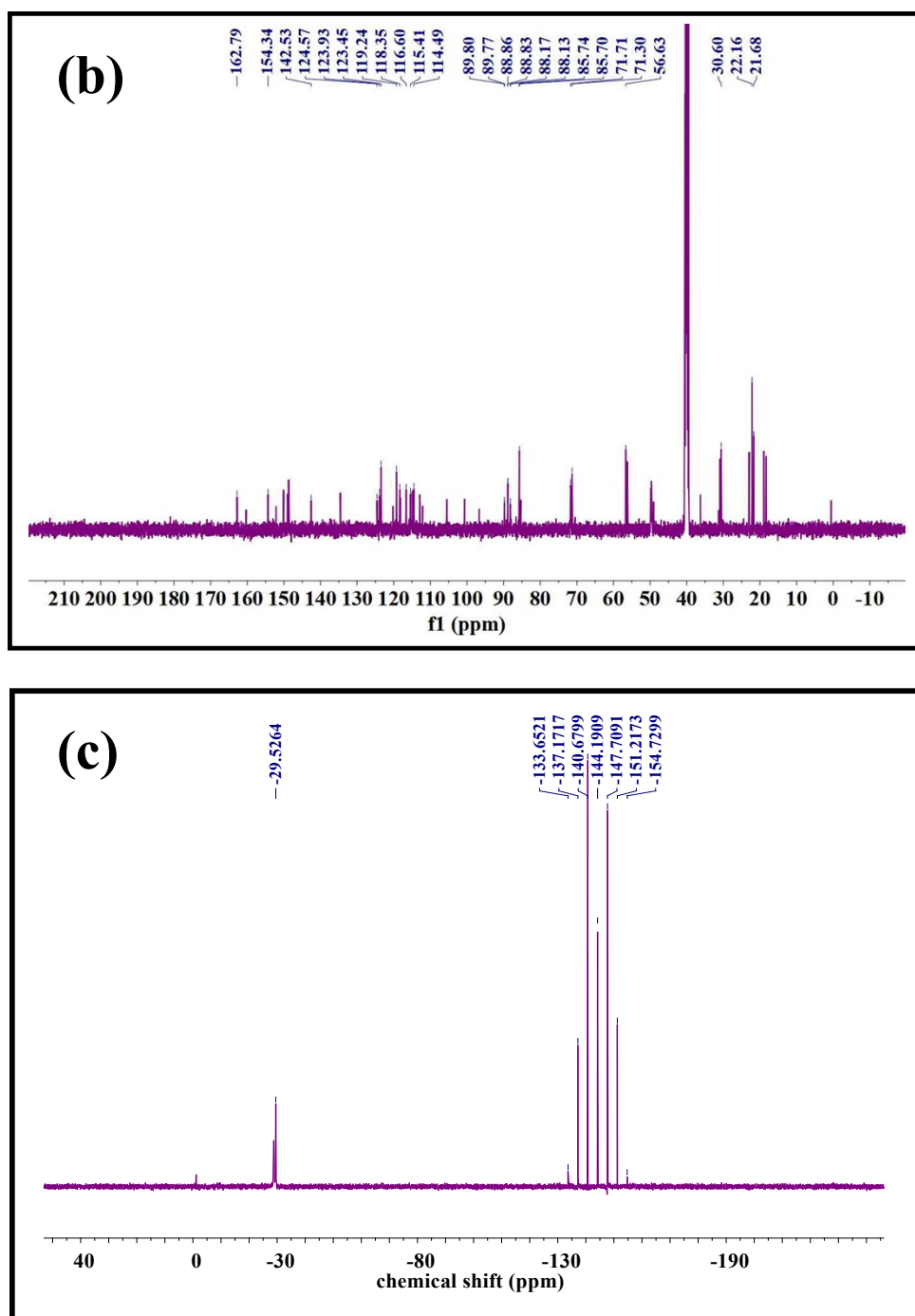


**Figure S4:** NMR spectra of Complex **3** in DMSO- $d_6$  (a)  $^1\text{H}$  NMR (b)  $^{13}\text{C}$  NMR (c)  $^{31}\text{P}$  NMR

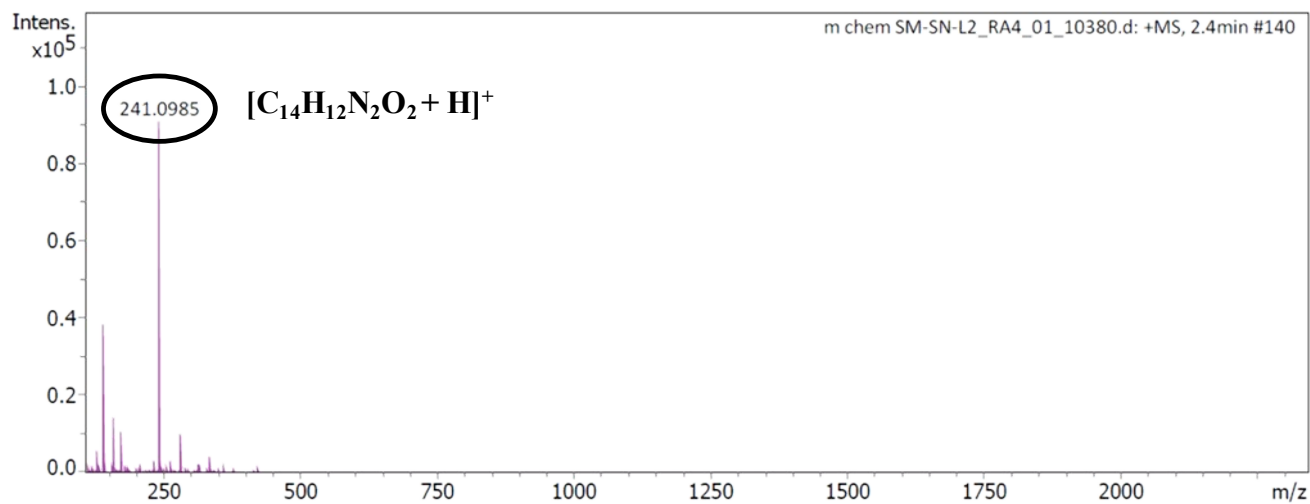


Figure S5: ESI-MS of ligand (HL)

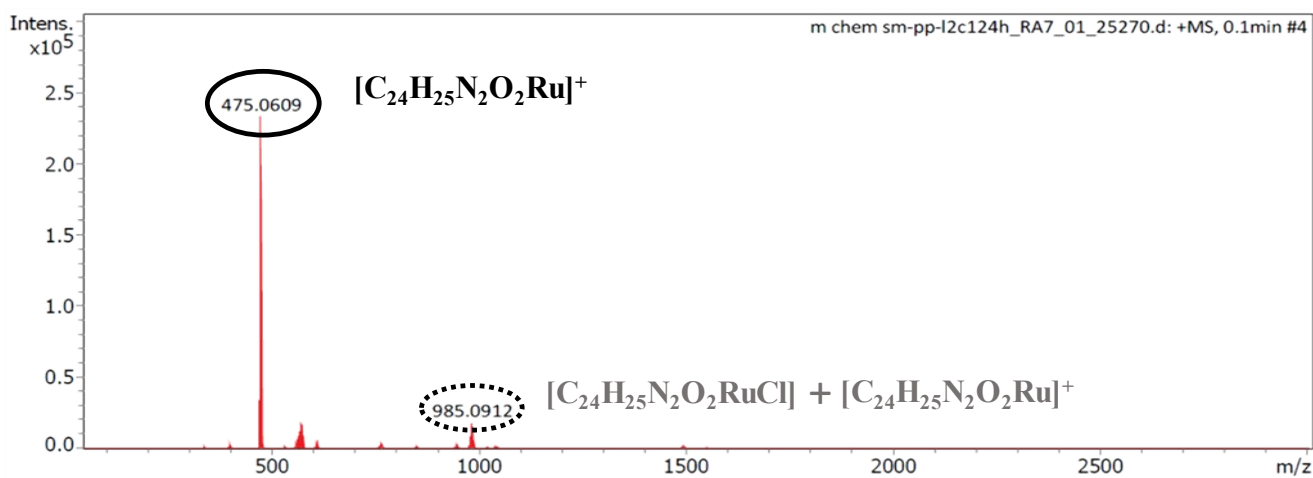


Figure S6: ESI-MS of complex 1

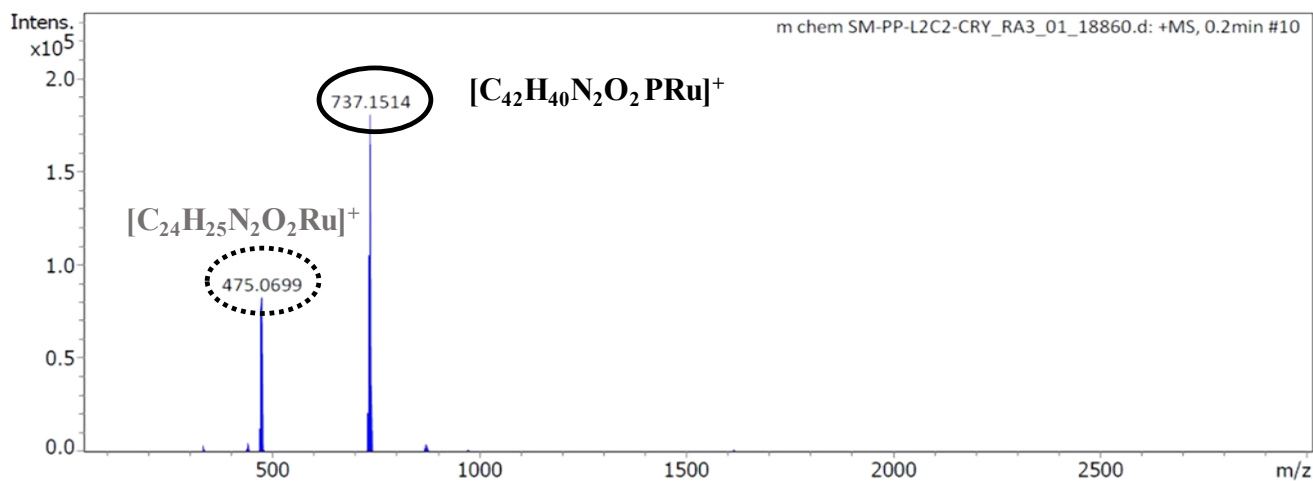


Figure S7: ESI-MS of complex 2

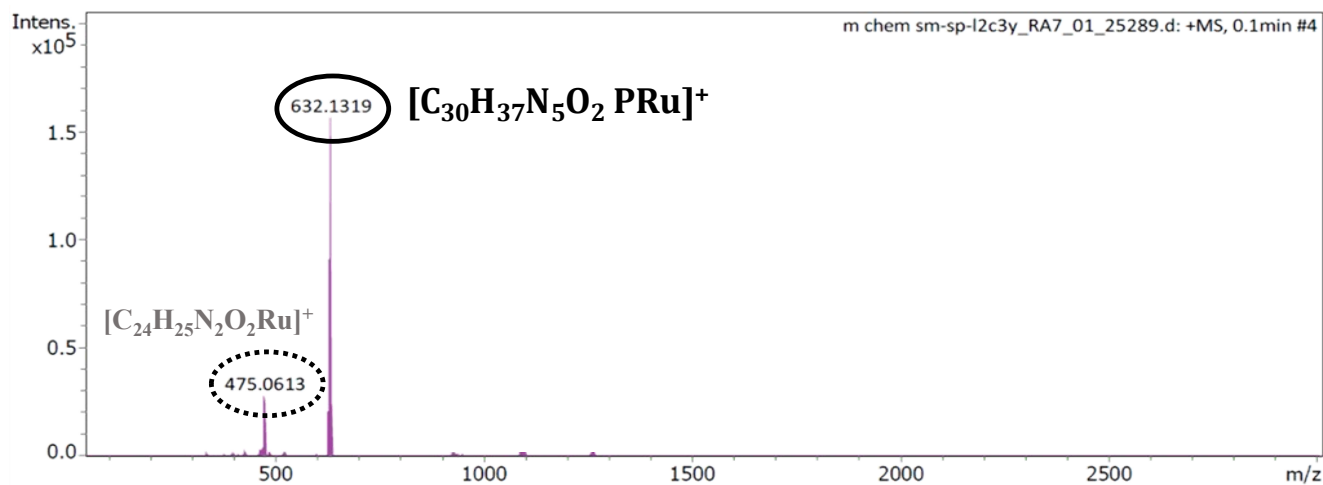


Figure S8: ESI-MS of complex 3

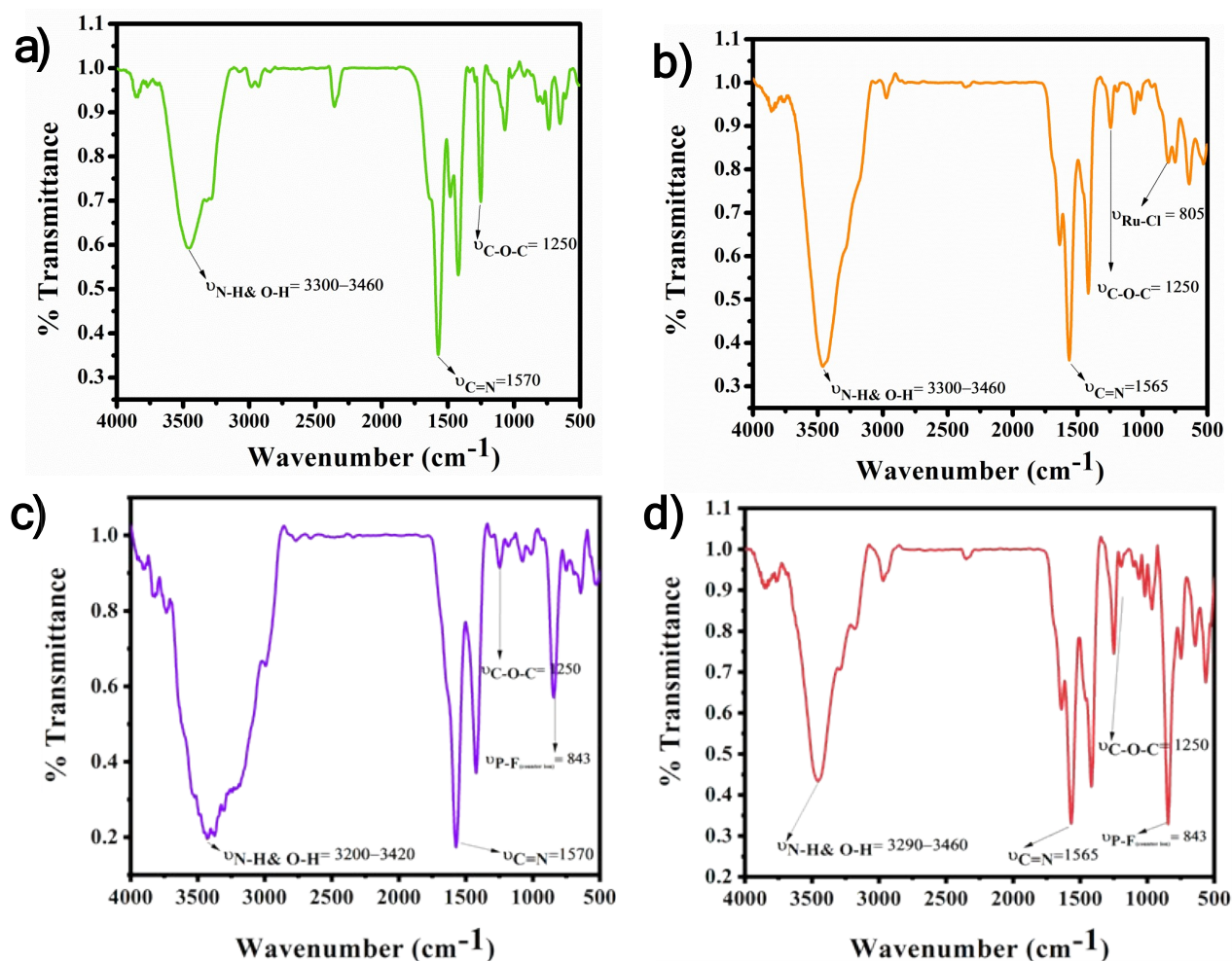
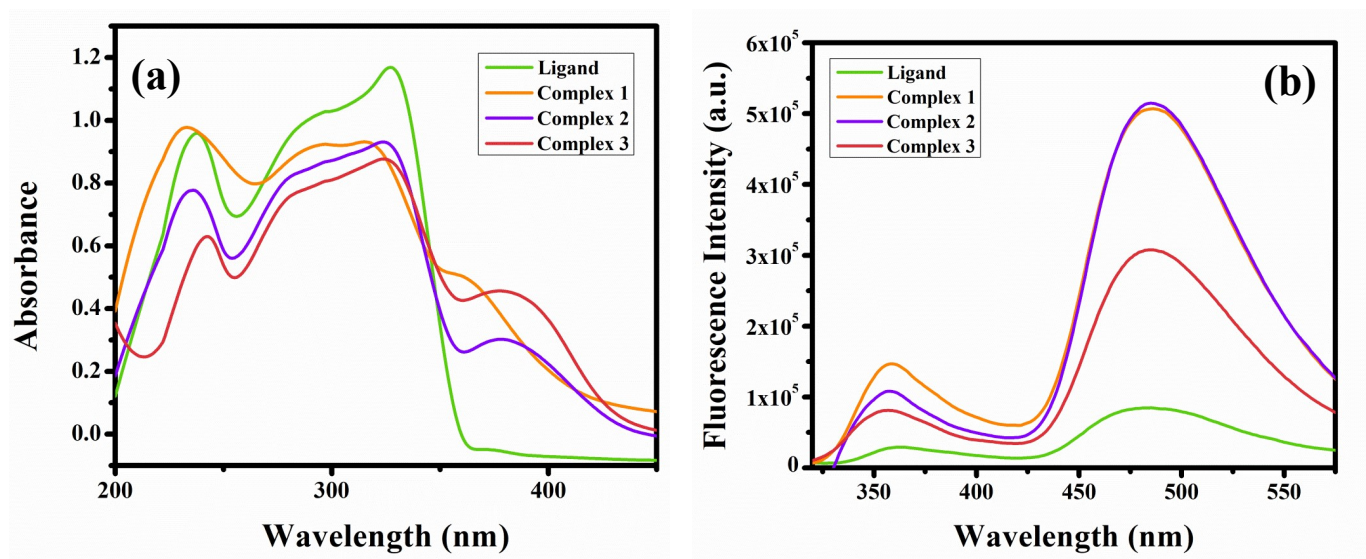
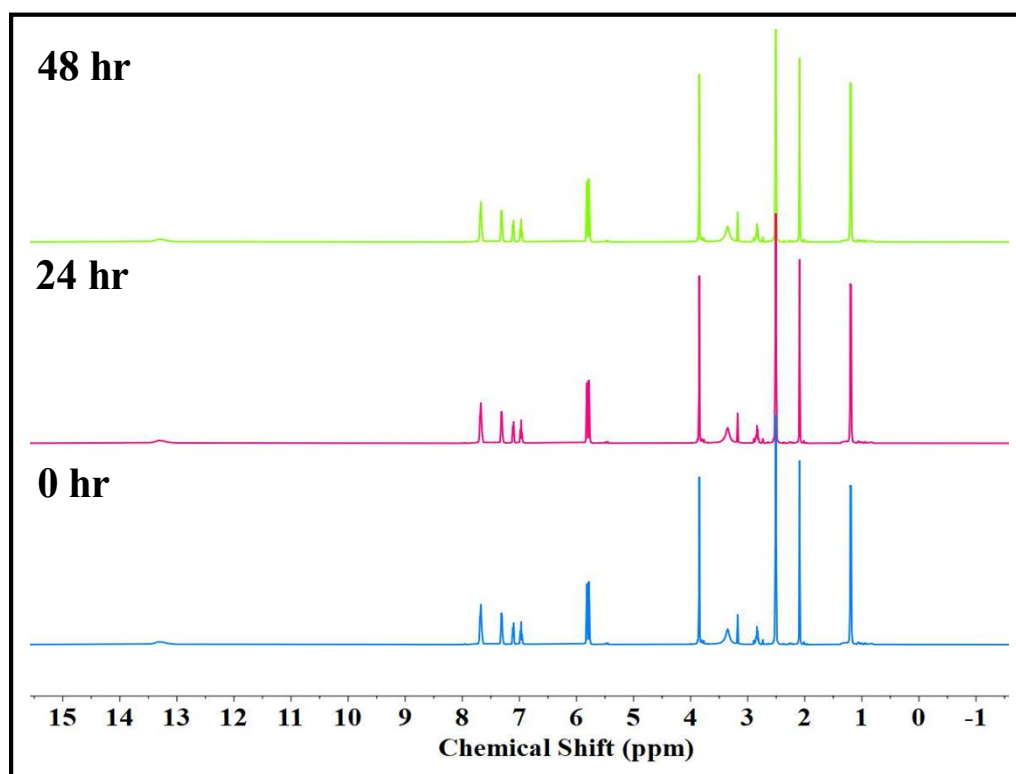


Figure S9: FTIR stretching frequencies (in KBr pellet) of (a) ligand (HL), (b) complex 1, (c) complex 2, and (d) complex 3



**FigureS10:** (a) UV-Visible spectra (b) emission spectra of ligand (HL) and complexes 1-3 in DMSO



**Figure S11:** Time dependent stability study of complex 1 at different time intervals 0 hr, 24 hr, 48 hr using NMR spectroscopy.

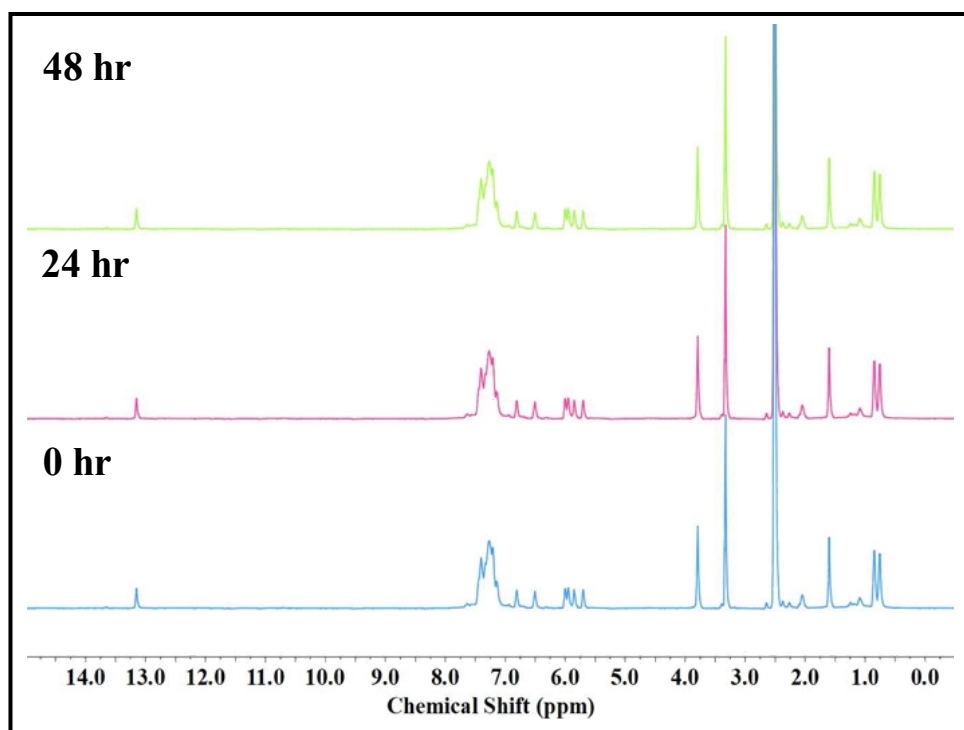


**Figure S12:** Time dependent stability study of complex **2** at different time intervals 0 hr, 24 hr, 48 hr using NMR spectroscopy.

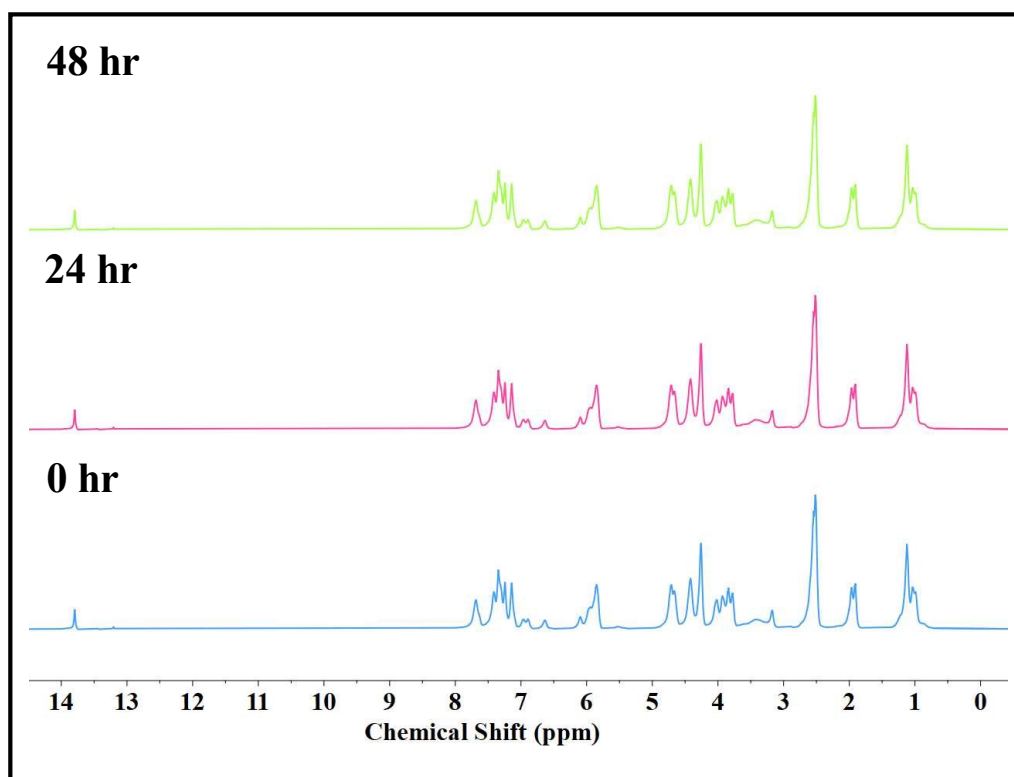


**Figure S13:** Time dependent stability study of complex **3** at different time intervals 0 hr, 24 hr, 48 hr using NMR spectroscopy.



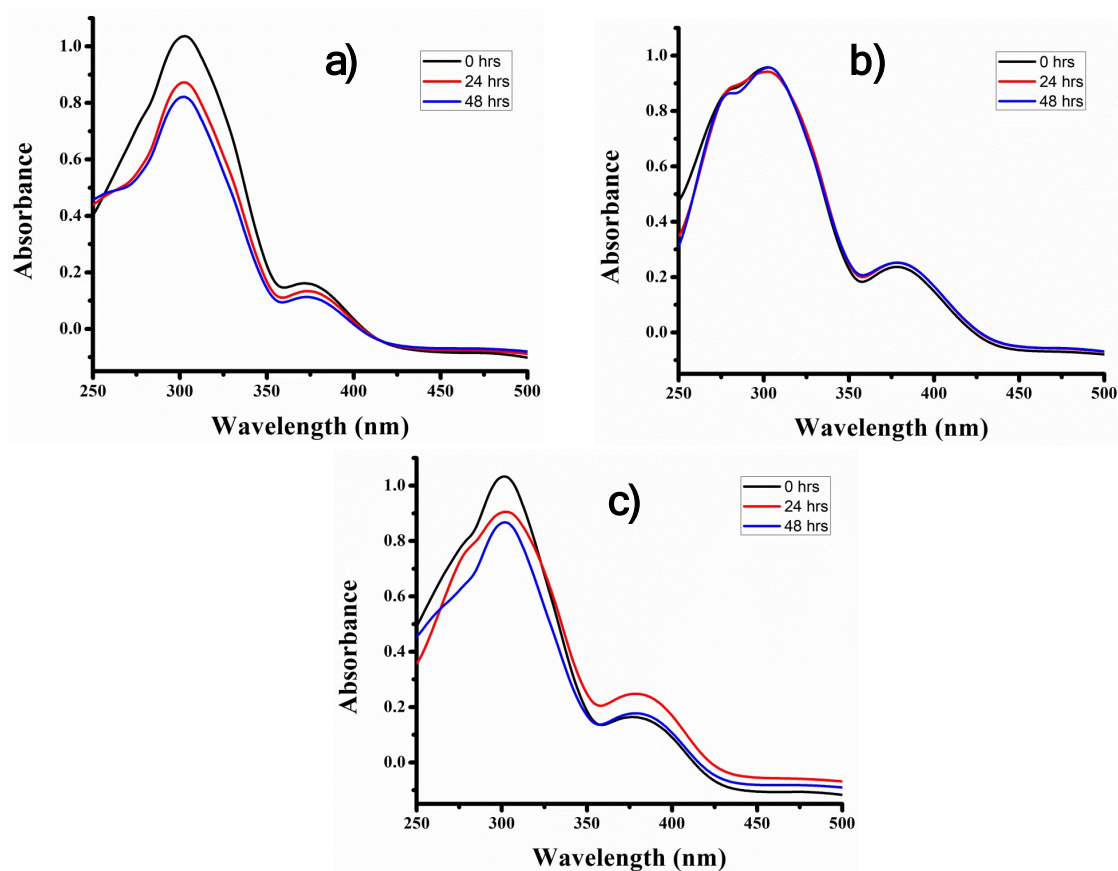


**Figure S14:** Stability study of the (a) complex **1**, (b) complex **2**, and (c) complex **3** (in 1% DMSO in PBS Solution) using UV spectroscopy

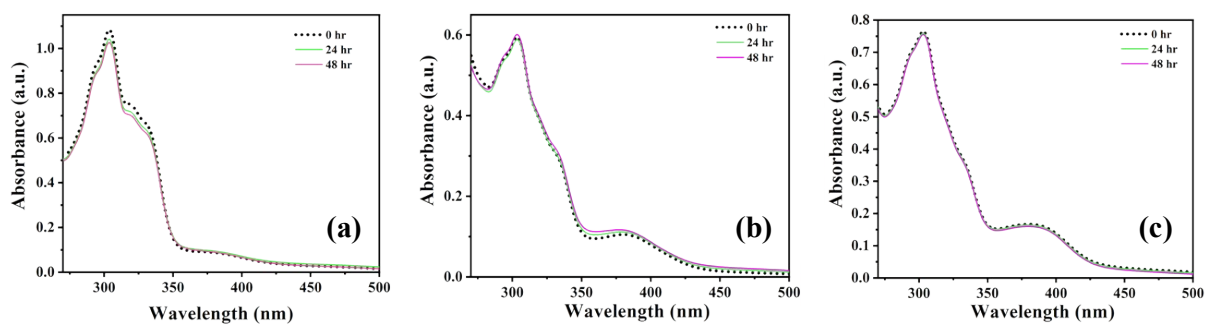


**Figure S15.** Stability study of complexes in biological medium (a) complex **1** (b) complex **2** (c) complex **3** at different time interval 0 hr, 24 hr, 48 hr (in DMEM).

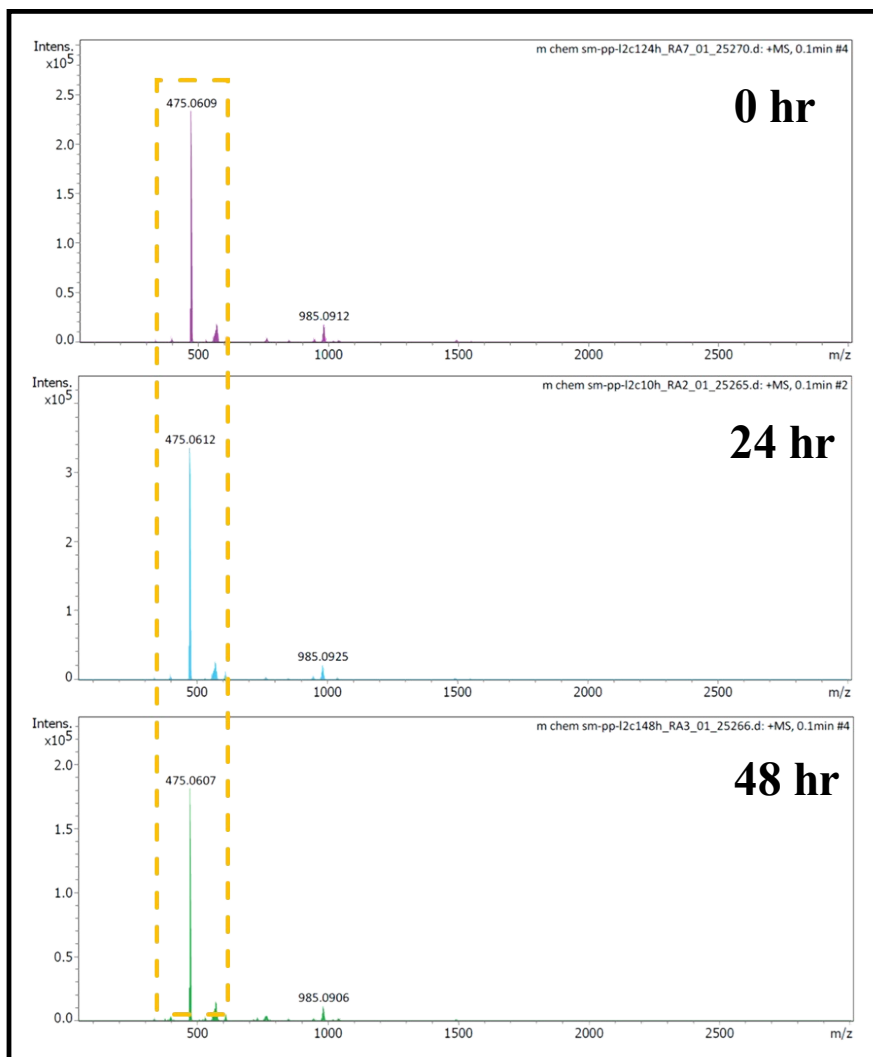


**Figure S16.** Stability study of complex **1** in biological medium at different time intervals 0 hr, 24 hr, 48 hr via LC-MS.

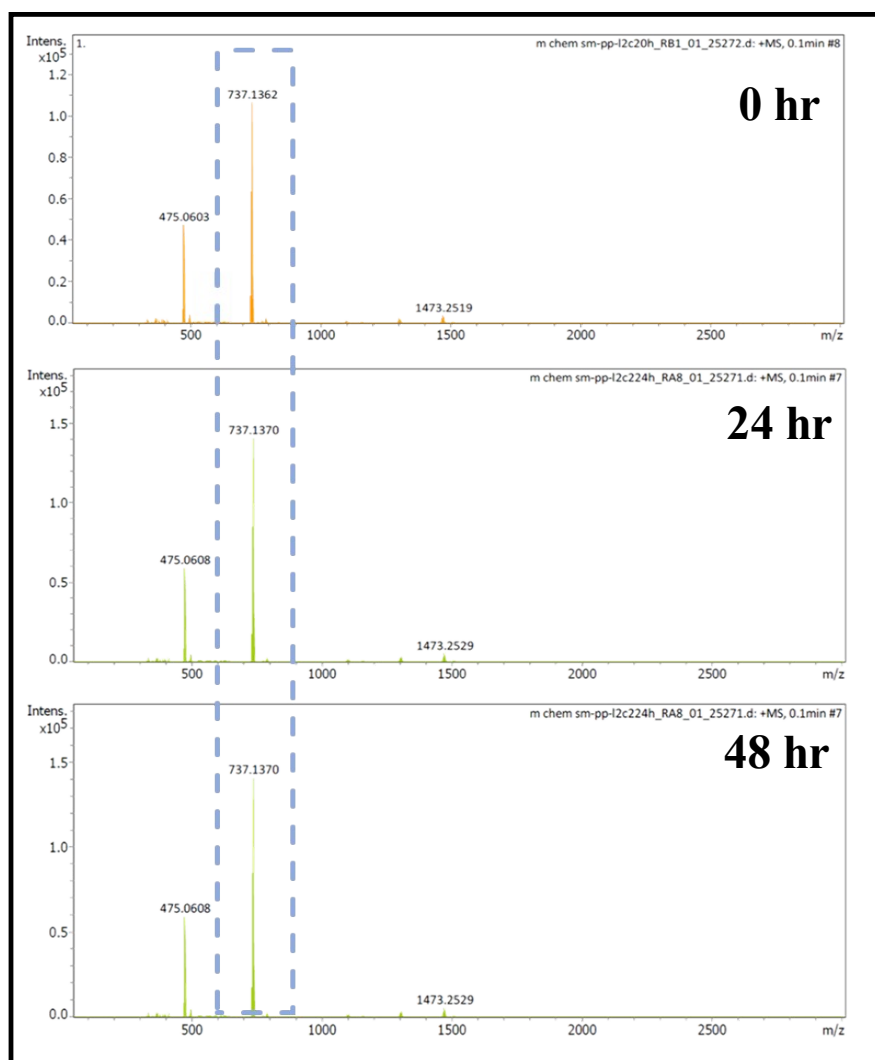


**Figure S17.** Stability study of complex 2 in biological medium at different time intervals 0 hr, 24 hr, 48 hr via LC-MS.

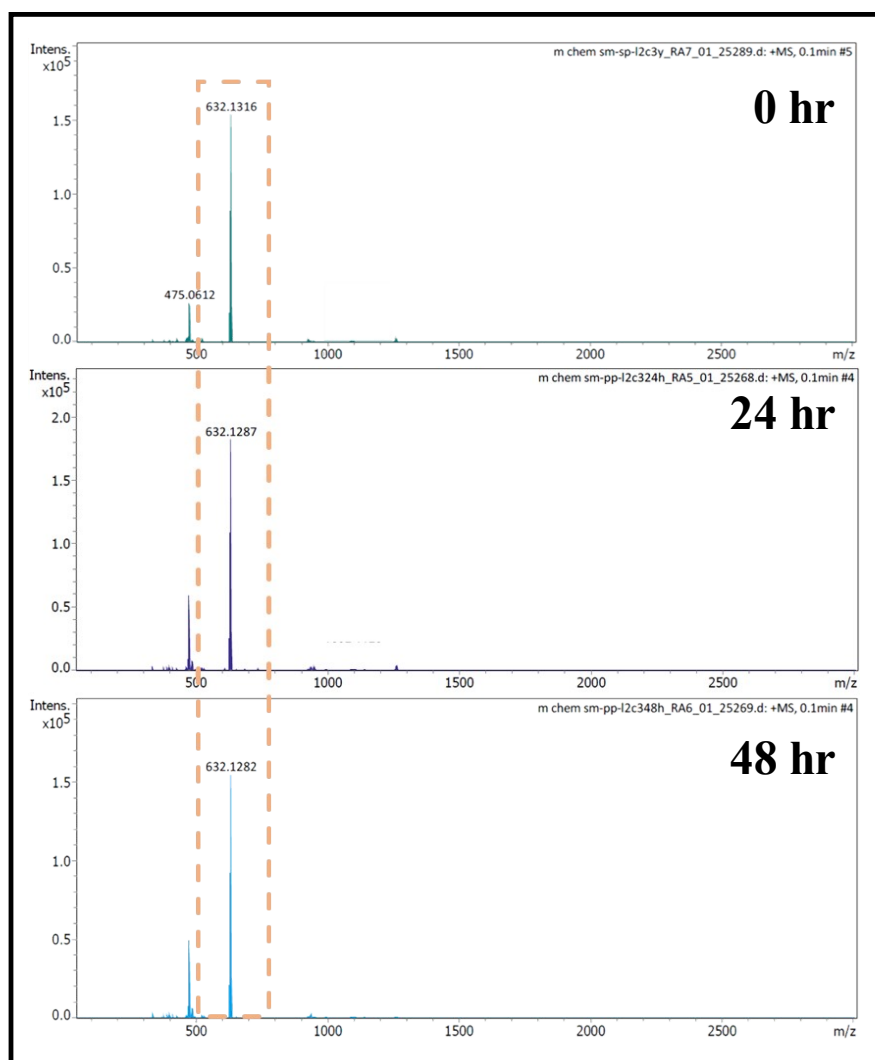


**Figure S18.** Stability study of complex **3** in biological medium at different time interval 0 hr, 24 hr, 48 hr via LC-MS.

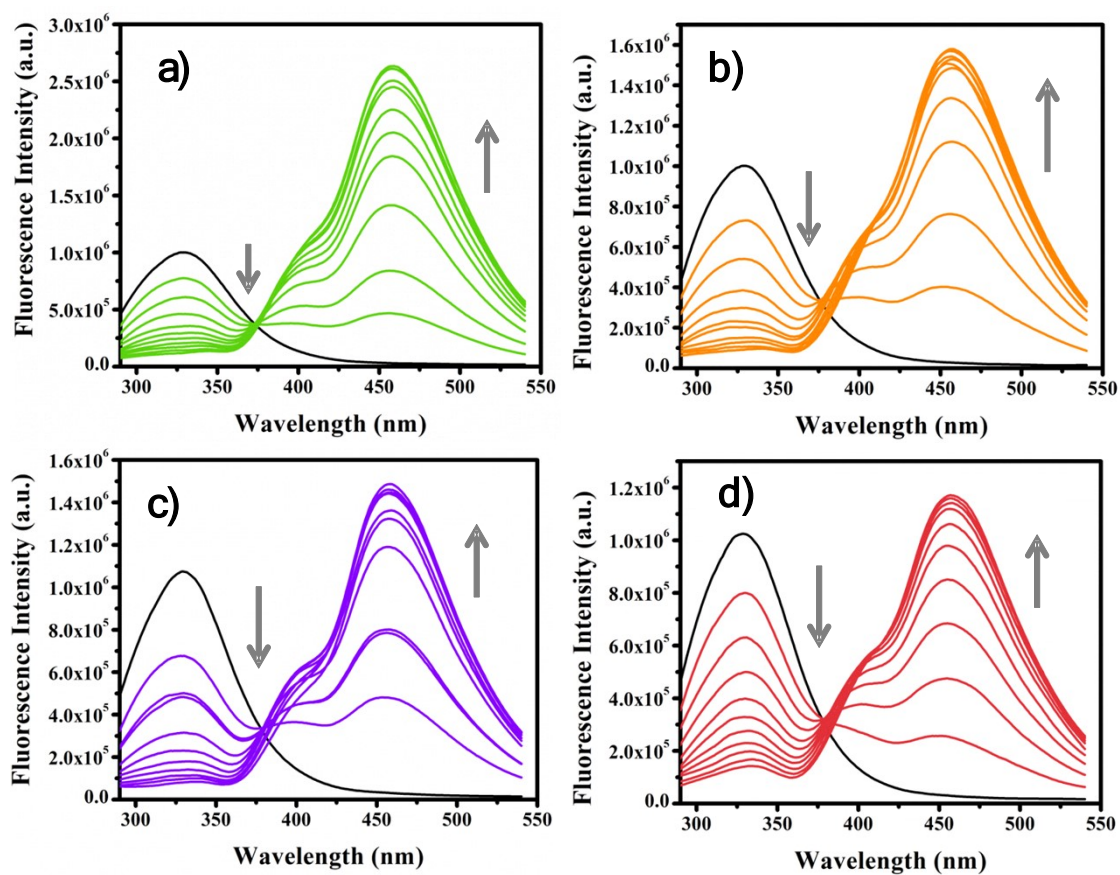


**Figure S19:** Fluorescence quenching spectra of HSA (10  $\mu\text{M}$ ) of (a) ligand (HL), (b) complex 1, (c) complex 2, and (d) complex 3 (2-20  $\mu\text{M}$ ) at 298 K.

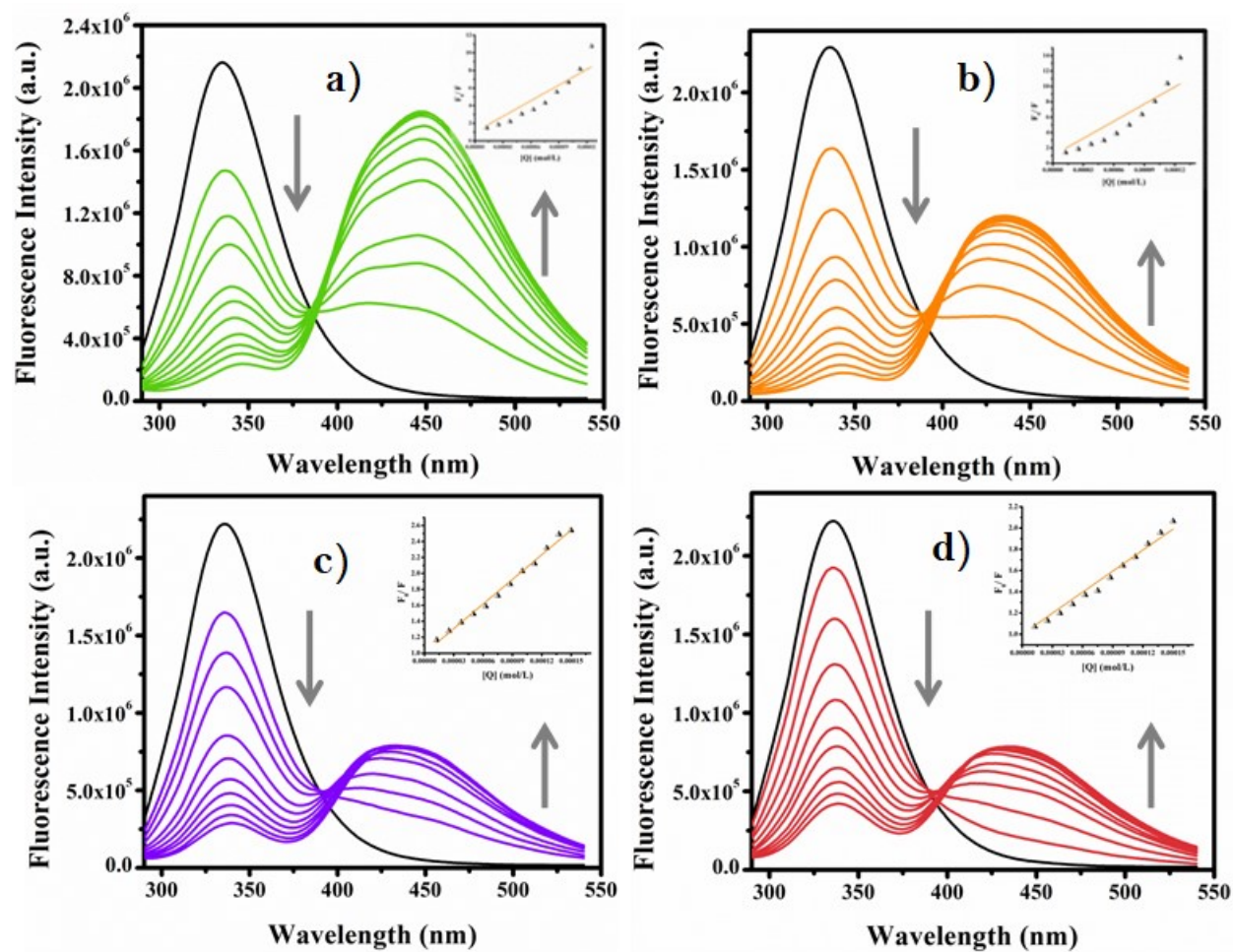


**Figure S20.** Fluorimetric titration spectra of BSA (10  $\mu$ M) in Tris-HCl buffer with (a) ligand (**HL**), (b) complex **1**, (c) complex **2**, and (d) complex **3** (2-20  $\mu$ M) at 298 K. Inset: Stern-Volmer plots for BSA.

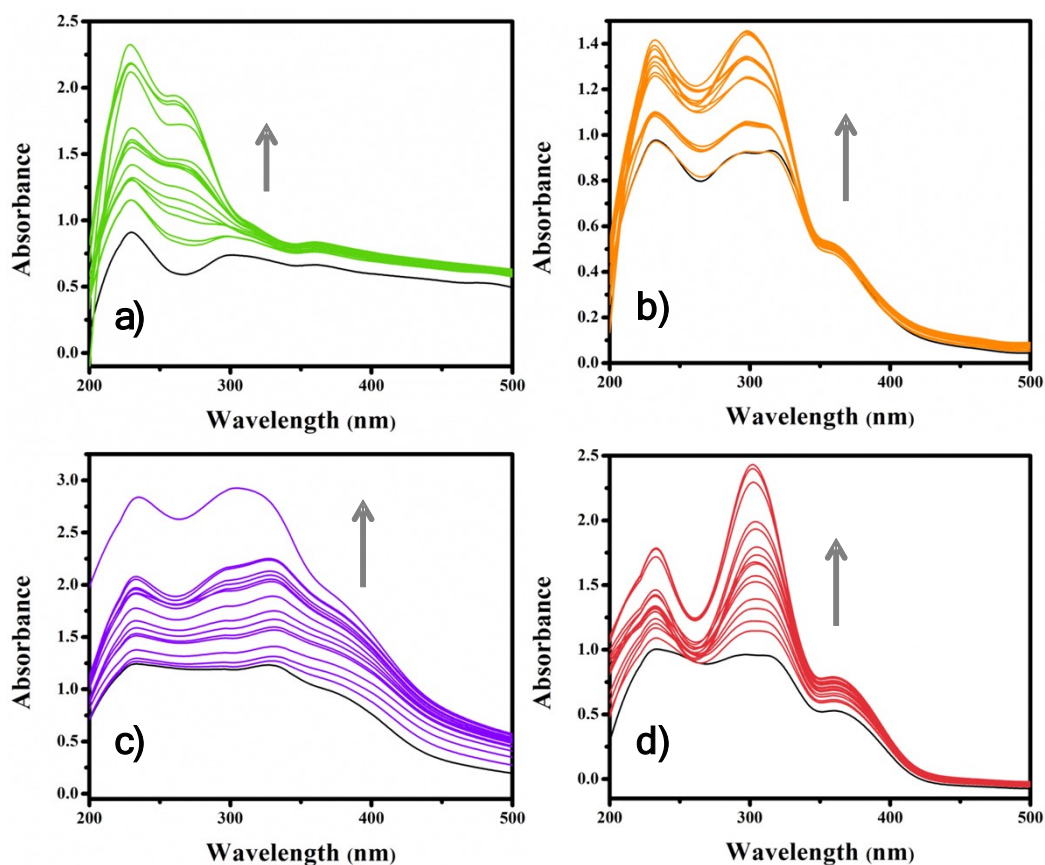


**Figure S21:** Absorption titration spectra of (a) ligand (HL), (b) complex 1, (c) complex 2, and (d) complex 3 with increasing concentrations of CT-DNA.

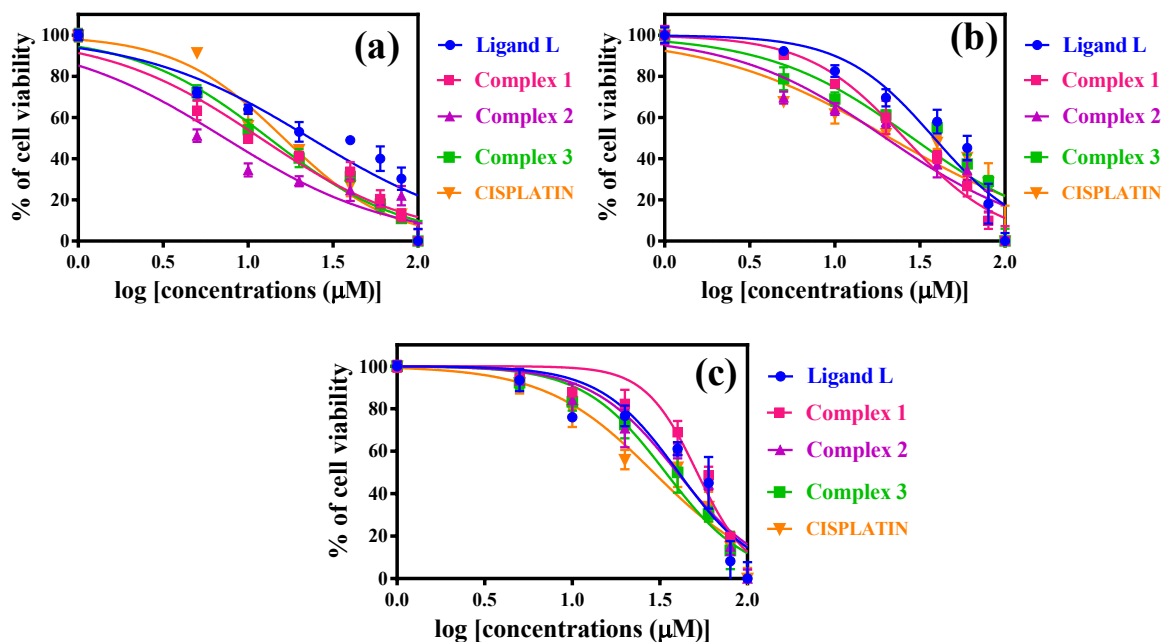


**Figure S22:** Normalized log of concentrations of the doses of ligand (HL) and complexes 1-3 against (a) HeLa, (b) MCF7 (cancer cell lines) and (c) HEK 293 (normal cell line).



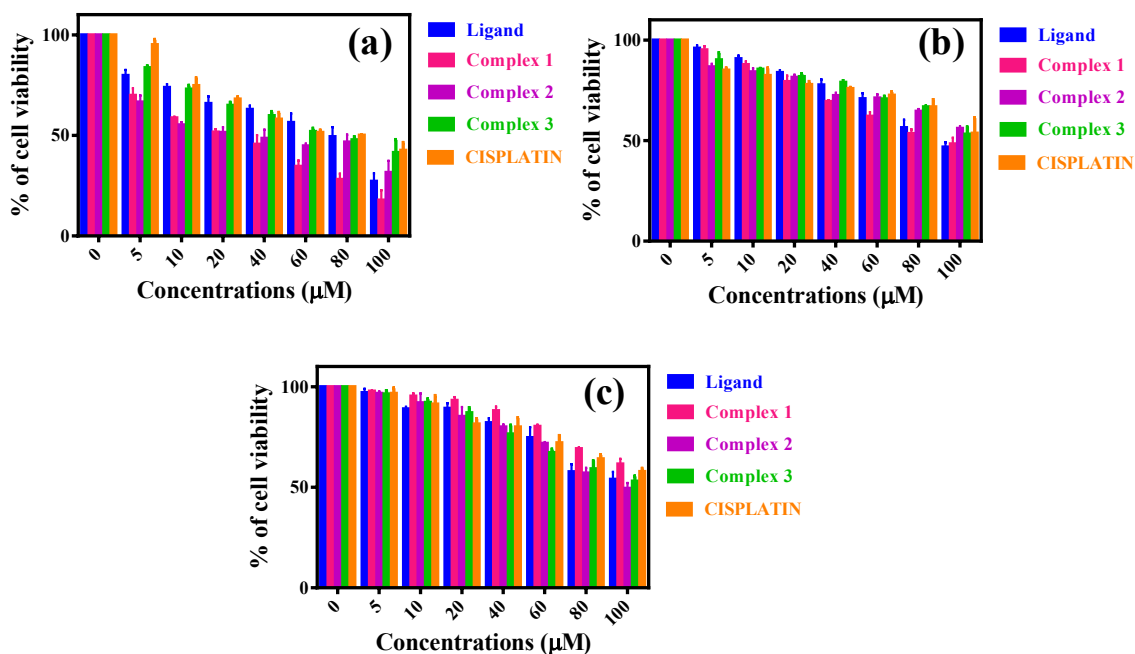


**Figure S23.** Cell viability curve for ligand (HL) and complexes 1-3 against cancer cell lines (a) HeLa, (b) MCF-7 and (c) normal cell line HEK 293.

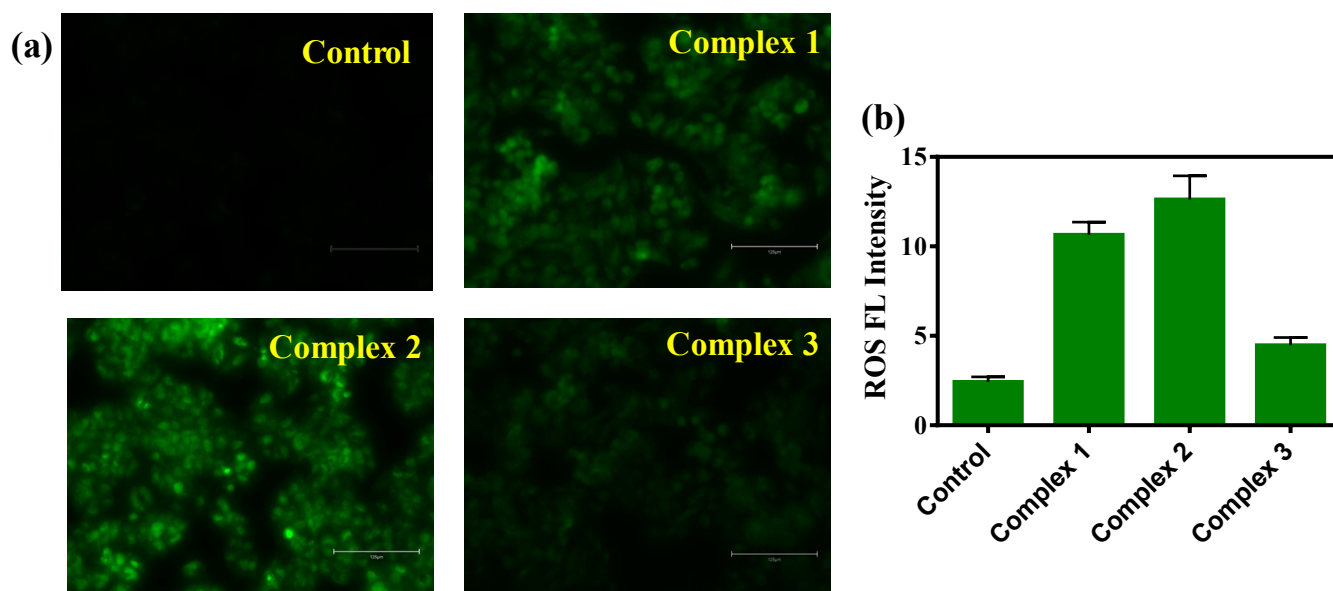


**Figure S24:** (a) Generation of reactive oxygen species after the treatment of complexes in HeLa cells (b) Histogram graph of ROS fluorescence intensity.



**Table S1:** Selected bond lengths (Å) and bond angles (°) of complexes **1** and **2**.

Complex 1		Complex 2	
<b>Ru1-Cl1</b>	2.4009(8)	<b>Ru1-P1</b>	2.3582(6)
<b>Ru1-O1</b>	2.081(2)	<b>Ru1-O1</b>	2.0576(15)
<b>Ru1-N1</b>	2.084(3)	<b>Ru1-N1</b>	2.1005(18)
<b>Ru1-C1</b>	2.199(3)	<b>Ru1-C1</b>	2.255(2)
<b>Ru1-C2</b>	2.189(3)	<b>Ru1-C2</b>	2.188(2)
<b>Ru1-C3</b>	2.174(3)	<b>Ru1-C3</b>	2.228(2)
<b>Ru1-C4</b>	2.200(3)	<b>Ru1-C4</b>	2.280(2)
<b>Ru1-C5</b>	2.173(3)	<b>Ru1-C5</b>	2.209(2)
<b>Ru1-C6</b>	2.183(3)	<b>Ru1-C6</b>	2.195(2)
<b>C17-N1</b>	1.339(4)	<b>C17-N1</b>	1.338(3)
<b>C16-N2</b>	1.378(4)	<b>C17-N2</b>	1.356(3)
<b>O1-Ru1-N1</b>	82.36(9)	<b>O1-Ru1-N1</b>	82.18(7)
<b>O1-Ru1-Cl1</b>	85.02(6)	<b>O1-Ru1-P1</b>	80.02(5)
<b>Cl1-Ru1-C1</b>	89.94(9)	<b>C1-Ru1-P1</b>	97.54(6)
<b>Cl1-Ru1-C2</b>	94.65(9)	<b>C2-Ru1-P1</b>	124.24(7)
<b>Cl1-Ru1-C3</b>	123.46(9)	<b>C3-Ru1-P1</b>	161.82(6)
<b>Cl1-Ru1-C4</b>	161.51(9)	<b>C4-Ru1-P1</b>	154.09(6)
<b>Cl1-Ru1-C5</b>	150.43(8)	<b>C5-Ru1-P1</b>	117.99(6)
<b>Cl1-Ru1-C6</b>	112.77(9)	<b>C6-Ru1-P1</b>	95.07(6)
<b>N1-Ru1-Cl1</b>	84.93(7)	<b>O1-Ru1-N1</b>	76.54(5)
<b>O1-Ru1-C1</b>	149.03(12)	<b>O1-Ru1-C1</b>	147.10(8)
<b>O1-Ru1-C2</b>	111.88(11)	<b>O1-Ru1-C2</b>	162.70(8)
<b>O1-Ru1-C3</b>	89.68(11)	<b>O1-Ru1-C3</b>	125.27(8)
<b>O1-Ru1-C4</b>	94.27(10)	<b>O1-Ru1-C4</b>	95.25(8)
<b>O1-Ru1-C5</b>	123.93(10)	<b>O1-Ru1-C5</b>	88.61(7)
<b>O1-Ru1-C6</b>	162.20(10)	<b>O1-Ru1-C6</b>	110.42(7)
<b>N1-Ru1-C1</b>	127.67(12)	<b>N1-Ru1-C1</b>	165.26(8)
<b>N1-Ru1-C2</b>	165.70(12)	<b>N1-Ru1-C2</b>	141.08(8)
<b>N1-Ru1-C3</b>	149.84(11)	<b>N1-Ru1-C3</b>	105.58(8)

<b>N1-Ru1-C4</b>	113.34(11)	<b>N1-Ru1-C4</b>	87.88(8)
<b>N1-Ru1-C5</b>	92.56(11)	<b>N1-Ru1-C5</b>	98.14(8)
<b>N1-Ru1-C6</b>	99.22(12)	<b>N1-Ru1-C6</b>	130.44(9)

**Table S2:** Excitation and emission wavelengths of ligand (HL) and complexes 1-3

<b>Compound</b>	<b>UV-Vis (nm)</b>	<b><math>\lambda_{\text{excitation}}</math> (nm)</b>	<b><math>\lambda_{\text{emission}}</math> (nm)</b>
<b>Ligand (HL)</b>	327, 238	327	363, 482
<b>Complex 1</b>	357, 320, 233	320	359, 486
<b>Complex 2</b>	378, 324, 236	324	358, 485
<b>Complex 3</b>	377, 324, 243	324	357, 484

**Table S3:** Various binding parameters analyzed from SV and Scatchard plots

<b>Compound</b>	<b><math>K_{\text{sv}}(\text{M}^{-1})</math></b>	<b><math>K_{\text{q}}(\text{M}^{-1}\text{s}^{-1})</math></b>	<b><math>K_{\text{a}}(\text{M}^{-1})</math></b>	<b>n</b>
<b>BSA</b>				
<b>Ligand (HL)</b>	$5.9 \times 10^4$	$9.5 \times 10^{12}$	$9.5 \times 10^5$	1.3
<b>Complex 1</b>	$4.6 \times 10^4$	$7.4 \times 10^{12}$	$1.1 \times 10^6$	1.35
<b>Complex 2</b>	$7.4 \times 10^4$	$1.1 \times 10^{13}$	$5.5 \times 10^6$	1.5
<b>Complex 3</b>	$2.9 \times 10^4$	$4.7 \times 10^{12}$	$1.9 \times 10^6$	1.45
<b>HSA</b>				
<b>Ligand (HL)</b>	$4.9 \times 10^4$	$7.9 \times 10^{12}$	$1.9 \times 10^6$	1.4
<b>Complex 1</b>	$6.7 \times 10^4$	$1.1 \times 10^{13}$	$3.6 \times 10^6$	1.43
<b>Complex 2</b>	$1.8 \times 10^5$	$2.9 \times 10^{13}$	$2.9 \times 10^7$	1.55
<b>Complex 3</b>	$4.3 \times 10^4$	$6.7 \times 10^{12}$	$1.1 \times 10^6$	1.35

**Table S4:** IC<sub>50</sub> values obtained from MTT assay of the ligand (**HL**) and complexes **1-3** against cancer cell lines (HeLa and MCF-7) along with a comparison with normal cell line (HEK 293).

Compound	IC <sub>50</sub> values			Selectivity Index	
	HeLa	MCF7	HEK-293	HeLa	MCF7
<b>Ligand</b>	23.22 ± 0.33	38.45 ± 0.68	40.42 ± 0.49	1.74	1.05
<b>Complex 1</b>	11.84 ± 0.42	25.67 ± 0.56	51.62 ± 0.27	4.35	2.01
<b>Complex 2</b>	7.29 ± 0.38	19.97 ± 0.39	39.73 ± 0.42	5.44	1.98
<b>Complex 3</b>	13.25 ± 0.35	28.70 ± 0.48	34.11 ± 0.47	2.57	1.18
<b>CISPLATIN</b>	16.20 ± 0.28	21.19 ± 0.66	29.13 ± 0.47	1.79	1.37

## References

1. Gaochao Lv, Liubin Guo, Ling Qiu, Hui Yang, Tengfei Wang, Hong Liu and Jianguo Lin, *Dalton Transactions*, **2015**, 44, 7324
2. Kumar Kundu, Pragti, S. M. Mobin and S. Mukhopadhyay, *Dalton Transactions*, **2020**, 49, 15481–15503.
3. Pragti, B. K. Kundu, C. Sonkar, R. Ganguly and S. Mukhopadhyay, *Polyhedron*, **2021**, 207, 115379.
4. M. Das, B. K. Kundu, R. Tiwari, P. Mandal, D. Nayak, R. Ganguly and S. Mukhopadhyay, *Inorg. Chim. Acta*, **2018**, 469, 111-122.
5. B. K. Kundu, Pragti, S. Biswas, A. Mondal, S. Mazumdar, S. M. Mobin and S. Mukhopadhyay, *Dalton Transactions*, **2021**, 50, 4848-4858.
6. B. K. Kundu, P. Mandal, B. G. Mukhopadhyay, R. Tiwari, D. Nayak, R. Ganguly and S. Mukhopadhyay, *Sensors and Actuators B: Chemical*, **2019**, 282, 347-358.